doi:10.1093/brain/awy288 BRAIN 2019: 142; 193–208 | 193

BRAIN
A JOURNAL OF NEUROLOGY

Longitudinal multimodal MRI as prognostic and diagnostic biomarker in presymptomatic familial frontotemporal dementia

Lize C. Jiskoot,[1,2] Jessica L. Panman,[1,2] Lieke H. Meeter,[1] Elise G.P. Dopper,[1,2,3] Laura Donker Kaat,[1,4] Sanne Franzen,[1] Emma L. van der Ende,[1] Rick van Minkelen,[5] Serge A.R.B. Rombouts,[2,6,7] Janne M. Papma[1] and John C. van Swieten[1]

See Boeve and Rosen (doi:10.1093/brain/awy314) for a scientific commentary on this article.

Developing and validating sensitive biomarkers for the presymptomatic stage of familial frontotemporal dementia is an important step in early diagnosis and for the design of future therapeutic trials. In the longitudinal Frontotemporal Dementia Risk Cohort, presymptomatic mutation carriers and non-carriers from families with familial frontotemporal dementia due to microtubule-associated protein tau (*MAPT*) and progranulin (*GRN*) mutations underwent a clinical assessment and multimodal MRI at baseline, 2-, and 4-year follow-up. Of the cohort of 73 participants, eight mutation carriers (three *GRN*, five *MAPT*) developed clinical features of frontotemporal dementia ('converters'). Longitudinal whole-brain measures of white matter integrity (fractional anisotropy) and grey matter volume in these converters ($n = 8$) were compared with healthy mutation carriers ('non-converters'; $n = 35$) and non-carriers ($n = 30$) from the same families. We also assessed the prognostic performance of decline within white matter and grey matter regions of interest by means of receiver operating characteristic analyses followed by stepwise logistic regression. Longitudinal whole-brain analyses demonstrated lower fractional anisotropy values in extensive white matter regions (genu corpus callosum, forceps minor, uncinate fasciculus, and superior longitudinal fasciculus) and smaller grey matter volumes (prefrontal, temporal, cingulate, and insular cortex) over time in converters, present from 2 years before symptom onset. White matter integrity loss of the right uncinate fasciculus and genu corpus callosum provided significant classifiers between converters, non-converters, and non-carriers. Converters' within-individual disease trajectories showed a relatively gradual onset of clinical features in *MAPT*, whereas *GRN* mutations had more rapid changes around symptom onset. *MAPT* converters showed more decline in the uncinate fasciculus than *GRN* converters, and more decline in the genu corpus callosum in *GRN* than *MAPT* converters. Our study confirms the presence of spreading predominant frontotemporal pathology towards symptom onset and highlights the value of multimodal MRI as a prognostic biomarker in familial frontotemporal dementia.

1 Department of Neurology, Erasmus Medical Center, Rotterdam, The Netherlands
2 Department of Radiology, Leiden University Medical Center, Leiden, The Netherlands
3 Department of Neurology, VU Medical Center, Amsterdam, The Netherlands
4 Department of Clinical Genetics, Leiden University Medical Center, Leiden, The Netherlands
5 Department of Clinical Genetics, Erasmus Medical Center, Rotterdam, The Netherlands
6 Institute of Psychology, Leiden University, Leiden, The Netherlands
7 Leiden Institute for Brain and Cognition, Leiden University, Leiden, The Netherlands

Correspondence to: Prof. dr. J.C. van Swieten
Erasmus Medical Center
Department of Neurology

Received February 2, 2018. Revised September 26, 2018. Accepted October 2, 2018. Advance Access publication November 30, 2018
© The Author(s) (2018). Published by Oxford University Press on behalf of the Guarantors of Brain.
This is an Open Access article distributed under the terms of the Creative Commons Attribution Non-Commercial License (http://creativecommons.org/licenses/by-nc/4.0/), which permits non-commercial re-use, distribution, and reproduction in any medium, provided the original work is properly cited. For commercial re-use, please contact journals.permissions@oup.com

Downloaded from https://academic.oup.com/brain/article-abstract/142/1/193/5225004 by Erasmus University Rotterdam user on 07 January 2019

's-Gravendijkwal 230, 3015 CE Rotterdam, The Netherlands
E-mail: j.c.vanswieten@erasmusmc.nl

Keywords: frontotemporal dementia; familial; presymptomatic; multimodal MRI; biomarkers

Abbreviations: (bv)FTD = (behavioural variant) frontotemporal dementia; DTI = diffusion tensor imaging; (nfv)PPA = (non-fluent agrammatic variant) primary progressive aphasia; NPI-Q = Neuropsychiatric Inventory

Introduction

Frontotemporal dementia (FTD) is the second most common presenile dementia disorder (onset <65 years), with a clinical profile of behavioural disturbances and/or language deterioration [behavioural variant (bv)FTD or primary progressive aphasia (PPA)] (Agosta *et al.*, 2012; Rohrer and Rosen, 2013; Frings *et al.*, 2014). FTD can have an autosomal dominant inheritance pattern, with mutations in the *GRN* or *MAPT* genes and the *C9orf72* repeat expansion as its three major causes (Warren *et al.*, 2013). Structural neuroimaging studies in symptomatic FTD have shown predominant grey matter volume loss of the prefrontal cortex, anterior temporal lobe, insula and anterior cingulate cortex early in the disease course, with atrophy increasing as the disease progresses (Seeley *et al.*, 2008; Whitwell *et al.*, 2009*a*, 2015; Piguet *et al.*, 2011). Studies now also suggest white matter integrity loss as a hallmark of FTD, exceeding grey matter atrophy in location and severity (Agosta *et al.*, 2012; Rohrer and Rosen, 2013; Frings *et al.*, 2014; Lam *et al.*, 2014). The uncinate fasciculus, connecting the orbitofrontal cortex, temporal pole, insula and amygdala, has been suggested as the key target of network-led neurodegeneration early in the disease process (Mahoney *et al.*, 2014; Oishi *et al.*, 2015; see also the literature review in the Supplementary material).

Comparable to studies in presymptomatic familial Alzheimer's (Bateman *et al.*, 2012; Benzinger *et al.*, 2013; Kinnunen *et al.*, 2018) and Huntington's disease (Tabrizi *et al.*, 2013; Harrington *et al.*, 2016), converging evidence from studies in familial FTD also demonstrates the presence of a presymptomatic stage, reflected in early changes in neuroimaging, cognition, blood, and CSF (Borroni *et al.*, 2008; Dopper *et al.*, 2014; Rohrer *et al.*, 2015; Jiskoot *et al.*, 2016, 2018*a*, *b*; Meeter *et al.*, 2016). White matter integrity loss of the uncinate fasciculus was found in the presymptomatic stage of both *MAPT* (Dopper *et al.*, 2014; Jiskoot *et al.*, 2018*b*), and *GRN* mutation carriers (Borroni *et al.*, 2008). Studies demonstrated gene-specific white matter integrity loss in the forceps minor in *MAPT* (Dopper *et al.*, 2014), and the inferior fronto-occipital fasciculus (Borroni *et al.*, 2008), and internal capsule (Jiskoot *et al.*, 2018*b*) in *GRN*. Grey matter volume loss was found in, amongst others, the frontal, temporal, insular, and cingulate cortices (Janssen *et al.*, 2005; Cruchaga *et al.*, 2009; Rohrer *et al.*, 2015). Cognitive and structural neuroimaging changes were identified from 5 to 10 years before estimated onset, respectively, with the first changes in *MAPT* being naming deficits and grey matter volume loss of the temporal lobe (hippocampus and amygdala), and the first changes in *GRN* being working memory deficits and grey matter volume loss of the insula (Rohrer *et al.*, 2015). Although these results suggest a pathophysiological cascade of events in the presymptomatic stage of familial FTD, interpretation of these changes is hampered by the fact that analyses are based on cross-sectional data, and therefore do not represent individual longitudinal trajectories (Bateman *et al.*, 2012; Schuster *et al.*, 2015). Moreover, these studies make use of estimated years to symptom onset as a proxy for actual symptom onset, which is commonly used in familial Alzheimer's disease (Bateman *et al.*, 2012; Ryman *et al.*, 2014; Kinnunen *et al.*, 2018). Estimated years to onset is, however, far less accurate in familial FTD, given the large variation in age at onset between and within families (van Swieten and Heutink, 2008). Recent longitudinal analyses on 4-year follow-up neuropsychological assessment data (Jiskoot *et al.*, 2018*a*) demonstrated subtle cognitive decline, starting 2 years prior to the development of clinical symptoms, suggesting a more sudden onset rather than a gradual acceleration when approaching the symptomatic disease stage. Longitudinal neuroimaging studies describing the trajectories of white matter integrity and grey matter volume loss in the presymptomatic stage of *MAPT* and *GRN* mutations are still lacking, but could provide valuable information on (i) imaging-based disease staging; (ii) characterization of disease trajectories; (iii) validation of prognostic biomarkers; and (iv) establishing the sensitivity of various neuroimaging techniques in early disease stages (Schuster *et al.*, 2015).

In this study, we investigated longitudinal changes in grey matter volume and white matter integrity over a 4-year follow-up period in mutation carriers that developed clinical features of FTD in this time window (converters), presymptomatic mutation carriers (non-converters), and non-carriers from Dutch FTD families with *GRN* or *MAPT* mutations. The study aims are threefold: (i) to investigate cross-sectional and longitudinal changes in white matter integrity and grey matter volume between converters, non-converters and non-carriers from 4 years before to symptom onset; (ii) to explore converters' within-individual trajectories; and (iii) to determine the prognostic value of longitudinal decline in multimodal neuroimaging parameters in predicting symptom onset, and to establish the best combination of multimodal neuroimaging parameters.

Downloaded from https://academic.oup.com/brain/article-abstract/142/1/193/5225004 by Erasmus University Rotterdam user on 07 January 2019

Materials and methods

Participants

A cohort of 83 participants with 50% risk of developing familial FTD, recruited between December 2009 and October 2012 from large Dutch families with *MAPT* or *GRN* mutations (Dopper *et al.*, 2014, 2016; Jiskoot *et al.*, 2016, 2018*a*), were followed on a 2-year basis over a time period of 4 years. DNA genotyping assigned participants either to the mutation carrier or non-carrier group: 43 mutation carriers (30 *GRN*, 13 *MAPT*) and 40 non-carriers (31 *GRN* family members, nine *MAPT* family members). At study entry, participants were asymptomatic according to established diagnostic criteria for bvFTD (Rascovsky *et al.*, 2011) or PPA (Gorno-Tempini *et al.*, 2011), with FTD Clinical Dementia Rating–sum of boxes (FTD-CDR-SB) scores of 0 (Knopman *et al.*, 2008). The study selection of mutation carriers was based on the presence of at least one follow-up MRI scan. We excluded 10 non-carriers who had not undergone all three study visits to ascertain stability of the data points, leaving 73 eligible participants in the final dataset (Fig. 1).

Standard protocol approvals, registrations, and patient consents

The clinical investigators and participants were blind for the participants' genetic status, except for those that underwent predictive testing at their own request. For converters, we offered genetic counselling to the patient and family members, and we unblinded the genetic status to confirm the presence of the pathogenic mutation. All participants gave written informed consent at study entry. The study was approved by the Medical and Ethical Review Committee of the Erasmus Medical Center.

Clinical assessment

Every 2 years, all participants underwent a standardized clinical assessment consisting of a brain MRI, medical history, neurological examination, and an extensive neuropsychological test battery. Knowledgeable informants (e.g. siblings, spouses) were asked about functional, cognitive, behavioural and/or neuropsychiatric changes by means of a structured interview, FTD-CDR-SB (Knopman *et al.*, 2008), and the Neuropsychiatric Inventory (NPI-Q), a well-validated questionnaire for neuropsychiatric features (Kaufer *et al.*, 2000), either during the study visit or afterwards in a telephone interview. Participants' depressive features were rated every study visit by means of the BDI (Beck *et al.*, 1961). Neuropsychological testing consisted of screening tests for global cognition—the Mini-Mental State Examination (MMSE; Folstein *et al.*, 1975) and Frontal Assessment Battery (FAB; Dubois and Litvan, 2000)—and tests within the domains of language, attention and mental processing speed, executive function, memory, visuoconstruction, and social cognition (see Jiskoot *et al.*, 2016, 2018*a* for the full battery).

Converters

Eight mutation carriers developed clinical features of FTD, five carrying an *MAPT* mutation and three carrying a *GRN* mutation. Using the information from the above-mentioned clinical

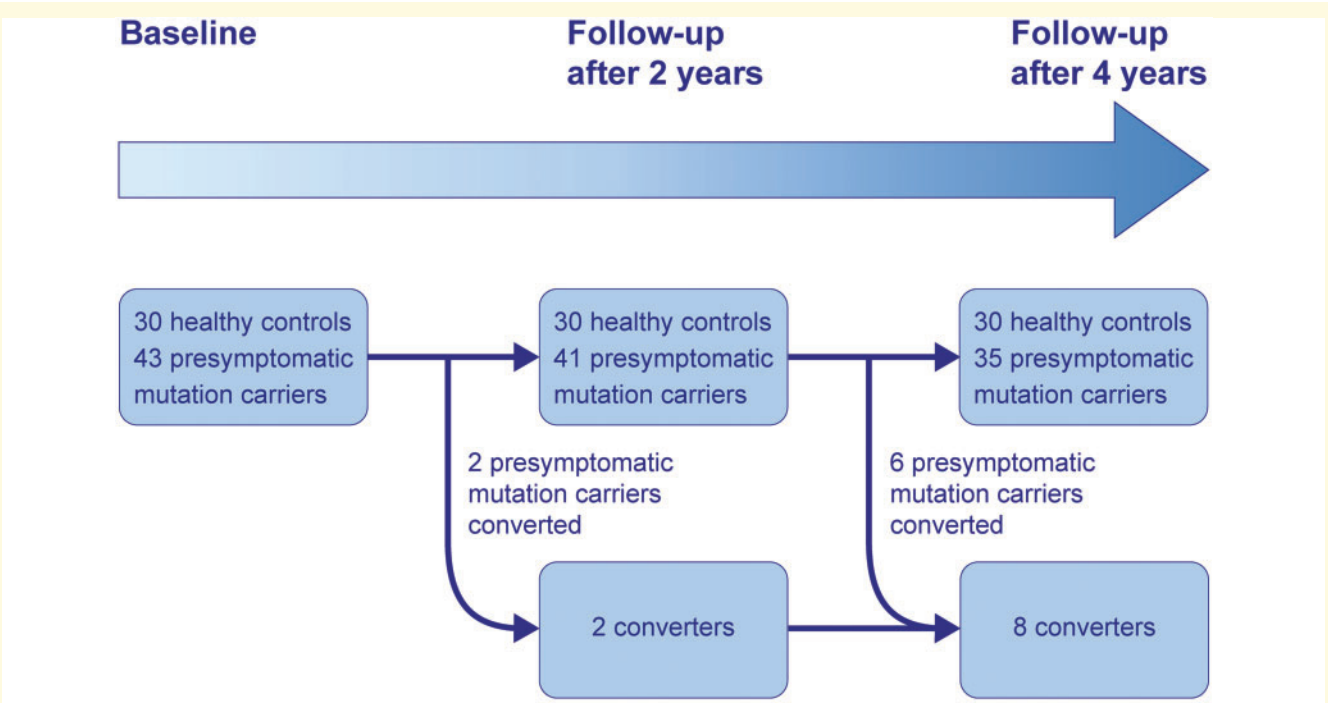

Figure 1 Study design. A schematic timeline of the 4-year follow-up of presymptomatic mutation carriers, converters and non-carriers within FTD-RisC. Eight mutation carriers converted to clinical FTD within the study window; two between baseline and follow-up after 2 years, and six between follow-up after 2 and 4 years. For the data analysis, the data were restructured into three new time points: 4 years before symptom onset, 2 years before symptom onset, and symptom onset.

Downloaded from https://academic.oup.com/brain/article-abstract/142/1/193/5225004 by Erasmus University Rotterdam user on 07 January 2019

assessment in a multidisciplinary consensus meeting of the Erasmus MC FTD Expertise Centre, we deemed mutation carriers to be converters (either bvFTD or PPA) if they met the following criteria: (i) progressive deterioration of behaviour and/or language by observation or history (as provided by a knowledgeable informant); (ii) significant functional decline (evidenced by FTD-CDR-SB scores $\geqslant 1$ at the first or second follow-up visit); and (iii) cognitive deficits [$\geqslant 1$ standard deviation (SD) in at least one domain] on neuropsychological assessment. The frontal and/or temporal atrophy on MRI in six converters (five *MAPT*, one *GRN*), together with progressive behaviour deterioration, functional decline, and cognitive deficits, met the international diagnostic consensus criteria (A–C) for probable bvFTD (Rascovsky *et al.*, 2011). The presence of predominant left posterior fronto-insular atrophy on MRI in two converters (both *GRN*), in combination with a non-fluent, halting speech, sound errors and agrammatism, impaired comprehension of syntactically complex sentences and spared single-word comprehension and object knowledge met the clinical diagnostic criteria for imaging-supported non-fluent/agrammatic variant PPA (nfvPPA; Gorno-Tempini *et al.*, 2011). The mutation carriers without clinical features of FTD (FTD-CDR-SB of 0 at all study visits) are referred to as 'non-converters' ($n = 35$). See Supplementary Table 1 and Supplementary material for demographic, neuroimaging, clinical and neuropsychological data of the converters, and Fig. 1 for converters' symptom onset within the study time-window.

Study design

The converters were compared to non-converters and non-carriers at three time points: baseline, follow-up after 2 and 4 years, presented as:

(i) 4 years before symptom onset: clinical and MRI data were available in six converters, as two developed symptoms between baseline and first follow-up visit, and therefore no data 4 years prior to symptom onset were available. Data were compared to baseline data of non-converters and non-carriers.

(ii) 2 years before symptom onset: clinical and MRI data were available for eight converters and compared to data of the 2-year follow-up of non-converters and non-carriers. Seven of the eight converters had reliable diffusion tensor imaging (DTI) data, while one converter (*MAPT*) was excluded due to insufficient data quality.

(iii) After symptom onset: clinical and MRI data were available from eight converters, and were compared to data of the follow-up after 4 years of non-converters and non-carriers. DTI data of seven converters were reliable, while one converter (*MAPT*) was excluded due to insufficient data quality.

Image acquisition and (pre)processing

On each study visit, we acquired volumetric T_1-weighted and diffusion tensor images on a Philips 3 T Achieva MRI scanner (Philips Medical Systems) using an 8-channel SENSE head coil. Images were preprocessed by means of standard FMRIB Software Library (FSL; version 5.0.6) voxel-based morphometry (VBM) and tract-based spatial statistics (TBSS) preprocessing tools (http://www.fmrib.ox.ac.uk/fsl). See the Supplementary material for specific image acquisition parameters and preprocessing pipelines. The resulting images were fed into whole-brain voxelwise statistics and region of interest analyses (see below).

Whole-brain voxelwise statistics: TBSS and VBM

We investigated cross-sectional white matter diffusion (fractional anisotropy) and grey matter volume differences between converters, non-converters and non-carriers at the three time points by means of permutation-based testing using 5000 permutations, applying one-way ANCOVAs with age and gender as covariates. Change over time maps were generated by subtracting the white matter and grey matter maps calculated at the post-symptom onset visit from the maps calculated at the 4 years before symptom onset visit in FSL. Using TFCE in Randomise, the significance level was set at family-wise error-corrected $P < 0.05$. As the field of view of the diffusion tensor images provided incomplete coverage of the lower brain areas including the cerebellum, the cerebellum was masked out from the TBSS analyses. In one of the converters we found a large (asymptomatic) cerebellar cyst, we therefore performed the VBM analyses in two steps, ascertaining that this subject did not significantly affect the results in the cerebellum: (i) the entire group with the cerebellum included in all subjects; and (ii) the analysis excluding the above-mentioned converter.

Region of interest selection

Based on an extensive literature search into white matter and grey matter changes in FTD (Supplementary material and Supplementary Table 2), we selected the following white matter regions of interest: uncinate fasciculus, superior longitudinal fasciculus, inferior longitudinal fasciculus, inferior fronto-occipital fasciculus, genu, body and splenium of the corpus callosum, fornix, cingulum bundle, and forceps minor. The John Hopkins University 1-mm atlas in FSL was used to parcel the entire white matter into predefined regions of interest (http://fsl.fmrib.ox.ac.uk/fsl/fslwiki/Atlases; Mori *et al.*, 2005). Using FSL tools, the regions of interest were restricted to voxels included in the mean fractional anisotropy skeleton mask, after which they were applied to the fractional anisotropy skeleton, giving left and right fractional anisotropy values per tract for each participant. The Harvard-Oxford 2-mm structural Atlas in FSL was applied to each subjects' native space grey matter segmentation, after which the mean voxel grey matter partial volume estimation per region (48 left, 48 right regions of interest) was multiplied with the total volume of the image (in $mm^3/1000$), giving the grey matter per region in millilitres. For the grey matter regions of interest, we selected the following regions: frontal lobe, prefrontal cortex, anterior temporal lobe, total temporal lobe, anterior cingulate cortex, total cingulate cortex, and insular cortex. The total cortical lobes and cingulate were the sum of all regions belonging to that area. The insula and anterior cingulate cortex were taken directly from the atlas. The prefrontal region of interest was the sum of the frontal pole, orbitofrontal cortex, and superior, middle and inferior frontal gyrus. The anterior temporal region of interest was the sum of the temporal pole and the

Downloaded from https://academic.oup.com/brain/article-abstract/142/1/193/5225004 by Erasmus University Rotterdam user on 07 January 2019

anterior divisions of the superior, middle and inferior temporal gyrus. All grey matter regions of interest were corrected for head size by expressing it as a percentage of the total intracranial volume in ml (%TIV), as automatically calculated in SPM12 (Wellcome Trust Centre for Neuroimaging, UCL, London, UK) running in MATLAB (version R2013b).

Statistical analysis

Statistical analyses were performed using SPSS Statistics 21.0 (IBM Corp., Armonk, NY) and GraphPad Prism 7 (La Jolla, California, USA). The significance level was set at $P < 0.05$ (two-tailed) across all comparisons. We compared baseline demographic data between groups by means of one-way ANOVA, with Bonferroni *post hoc* testing. Between-group differences in sex were analysed using Pearson χ^2 tests. We analysed longitudinal data points of global cognition and questionnaires using linear mixed models. We investigated the classification abilities of region of interest white matter integrity and grey matter volume loss to discriminate between converters, non-converters and non-carriers by determining the area under the curve with 95% confidence intervals obtained by receiver operating characteristic analyses, with optimal cut-off levels at the highest Youden's index (sensitivity + specificity – 1; Youden, 1950). First, for ease of interpretation, we standardized all raw fractional anisotropy and grey matter volumes by converting them into z-scores per time point (i.e. raw score minus the mean of non-carriers, divided by the standard deviation of non-carriers). Then, we calculated delta z-scores between time points per region of interest (after onset minus 4 years before symptom onset). To assess the performance of combinations of neuroimaging parameters, we performed logistic regression analyses, taking group (converter versus non-converter and converter versus non-carrier) as dependent variable and the delta z-scores as independent variables. The models were selected with a forward stepwise method according to the likelihood ratio test and by applying the standard *P*-values for variable inclusion (0.05) and exclusion (0.10), with age and gender as covariates. Goodness of fit was evaluated with the Hosmer-Lemeshow χ^2 test. Nagelkerke R^2 is reported as measure of effect size. To examine the converters' within-individual trajectories, we converted the raw clinical data scores to z-scores (i.e. individual test score minus the baseline mean of the non-carriers, divided by the baseline standard deviation of non-carriers) per time point. We calculated composite z-scores for cognitive domains by calculating z-scores per test and averaging the z-scores of the individual tests per domain (see Jiskoot *et al.*, 2016, 2018*a* for the neuropsychological assessment battery).

Data availability

The data that support the findings of this study are available on request from the corresponding author. The data are not publicly available as they contain information that could compromise the privacy of research participants (e.g. their mutation carriership).

Results

Demographics and clinical data

Demographic and clinical data of converters, non-converters and non-carriers are shown in Table 1. The mean familial age at symptom onset in converters was lower than in non-converters and non-carriers (both $P = 0.006$). After symptom onset, converters had lower MMSE scores than non-converters and non-carriers (both $P < 0.001$) and

Table 1 Demographics and clinical data

Demographic		Converters (*n* = 8)	Non-converters (*n* = 35)	Non-carriers (*n* = 30)	*P*-value
Age at study entry, years		49.5 ± 9.6	50.3 ± 10.2	50.6 ± 10.7	0.966
Sex, female (%)		4 (50)	21 (60)	19 (63.3)	0.790
Education (Verhage)[a]		6.0 ± 0.6	5.5 ± 1.0	5.4 ± 1.0	0.365
Gene, *GRN* (%)		3 (37.5)	27 (77.1)	24 (80)	0.050
Onset age family, years		52.4 ± 7.0	59.2 ± 5.5	59.4 ± 4.7	0.005
Years from estimated onset at study entry		5.0 ± 4.7	8.9 ± 8.1	N/A	0.596
Clinical data	**Years to onset**				
MMSE	4	29.3 ± 0.8	29.2 ± 1.5	29.4 ± 0.9	0.685
	2	29.1 ± 1.1	28.8 ± 1.9	29.4 ± 1.1	0.288
	0	26.3 ± 3.3	29.3 ± 1.2	29.4 ± 0.9	<0.001
FAB[b]	4	-	-	-	-
	2	17.3 ± 0.8	17.5 ± 0.9	17.5 ± 0.8	0.888
	0	15.7 ± 1.6	17.1 ± 1.1	16.9 ± 1.4	0.057
BDI	4	1.3 ± 1.6	3.5 ± 4.8	4.0 ± 4.3	0.414
	2	3.1 ± 3.9	3.2 ± 4.2	3.7 ± 4.1	0.897
	0	9.6 ± 10.5	3.0 ± 6.6	3.5 ± 4.3	0.032
NPI-Q[b]	4	-	-	-	-
	2	0.1 ± 0.4	2.9 ± 13.6	0.7 ± 1.3	0.638
	0	13.6 ± 16.4	3.9 ± 12.2	0.8 ± 1.5	0.015

Values indicate: mean ± SD. BDI = Beck's Depression Inventory; FAB = Frontal Assessment Battery; MMSE = Mini-Mental State Examination.
[a]Dutch educational system categorized into levels from 1 = <6 years of primary education to 7 = academic schooling (Verhage *et al.*, 1964).
[b]Data only available on follow-up visits.

Downloaded from https://academic.oup.com/brain/article-abstract/142/1/193/5225004 by Erasmus University Rotterdam user on 07 January 2019

significantly more neuropsychiatric features, reflected in higher BDI ($P = 0.031$ and $P = 0.054$, respectively) and NPI-Q ($P = 0.075$ and $P = 0.011$, respectively) scores. In longitudinal analyses, converters showed a significant decrease in MMSE over time ($P = 0.002$). Changes in global cognition or neuropsychiatric features did not reach statistical significance in non-converters and non-carriers, although somewhat higher NPI-Q scores were found in non-converters at 2- and 4-year follow-up.

Cross-sectional whole brain white matter integrity and grey matter volume loss

Four years before symptom onset, converters did not show any differences in fractional anisotropy or grey matter volume compared to non-converters and non-carriers [Table 2 and Fig. 2A(i)]. Two years before symptom onset, converters had lower fractional anisotropy values

Table 2 Whole brain comparisons (TBSS, VBM) between converters, non-converters and non-carriers

	WM/GM	Cluster	Size	*P*	MNI coordinates			L/R	Area (peak voxel)
					x	*y*	*z*		
Converters versus non-converters									
4 years before symptom onset	WM	-	-	ns	-	-	-	-	-
	GM	-	-	ns	-	-	-	-	-
2 years before symptom onset	WM	1	21781	0.004	15	42	–12	R	IFOF, UF, forceps minor
		2	1882	0.023	34	1	–32	R	Cingulum
		3	144	0.047	48	–36	–4	R	SLF
		4	66	0.049	–48	–10	22	L	SLF
		5	19	0.050	–56	0	15	L	SLF
	GM	1	27122	<0.001	10	12	–28	R	Orbitofrontal cortex
		2	4660	0.004	–40	2	–26	L	Planum temporale
After symptom onset	WM	1	61066	<0.001	35	–8	–37	R	ILF
	GM	1	88222	<0.001	50	–12	–46	R	Inferior temporal gyrus
Longitudinal decline	WM	1	894	0.047	–3	153	84	n/a	gCC
	GM	1	18601	0.001	–30	22	2	L	Insula
		2	6318	0.001	44	–32	–26	R	Inferior temporal gyrus
Converters versus non-carriers									
4 years before symptom onset	WM	-	-	ns	-	-	-	-	-
	GM	-	-	ns	-	-	-	-	-
2 years before symptom onset	WM	1	21781	0.004	15	42	–12	R	IFOF, UF, forceps minor
		2	1882	0.023	34	1	–32	R	Cingulum
		3	144	0.047	48	–36	–4	R	SLF
		4	66	0.049	–48	–10	22	L	SLF
		5	19	0.050	–56	0	15	L	SLF
	GM	1	23126	<0.001	40	–38	–30	R	Fusiform gyrus
		2	538	0.021	–16	50	32	L	Frontal pole
After symptom onset	WM	1	62308	<0.001	14	50	–15	R	IFOF, UF
	GM	1	81558	<0.001	42	–10	–48	R	Inferior temporal gyrus
		2	439	0.030	–14	–62	44	L	Precuneus
		3	150	0.036	–18	–78	–4	L	Lingual gyrus
		4	41	0.047	20	–86	–4	R	Occipital fusiform gyrus
Longitudinal decline	WM	1	914	0.026	–2	153	84	n/a	gCC
	GM	1	25216	0.001	–44	6	–30	L	Temporal pole
		2	11300	0.001	46	–32	28	R	Inferior temporal gyrus
		3	1165	0.014	18	–88	12	R	Occipital pole
		4	391	0.029	–34	–70	22	L	Lateral occipital cortex
		5	82	0.046	–20	–90	–4	L	Occipital pole
Non-converters versus non-carriers									
4 years before symptom onset	WM	-	-	ns	-	-	-	-	-
	GM	-	-	ns	-	-	-	-	-
2 years before symptom onset	WM	-	-	ns	-	-	-	-	-
	GM	-	-	ns	-	-	-	-	-
After symptom onset	WM	-	-	ns	-	-	-	-	-
	GM	-	-	ns	-	-	-	-	-
Longitudinal decline	WM	-	-	ns	-	-	-	-	-
	GM	-	-	ns	-	-	-	-	-

gCC = genu corpus callosum; GM = grey matter; IFOF = inferior fronto-occipital fasciculus; ILF = inferior longitudinal fasciculus; L = left; MNI = Montreal Neurological Institute; n/a = not applicable; ns = non-significant; R = right; SLF = superior longitudinal fasciculus; TBSS = Tract-Based Spatial Statistics; UF = uncinate fasciculus; VBM = voxel-based morphometry; WM = white matter. Clusters >50 voxels have been reported. $P < 0.05$, FWE-corrected for multiple comparisons.

Downloaded from https://academic.oup.com/brain/article-abstract/142/1/193/5225004 by Erasmus University Rotterdam user on 07 January 2019

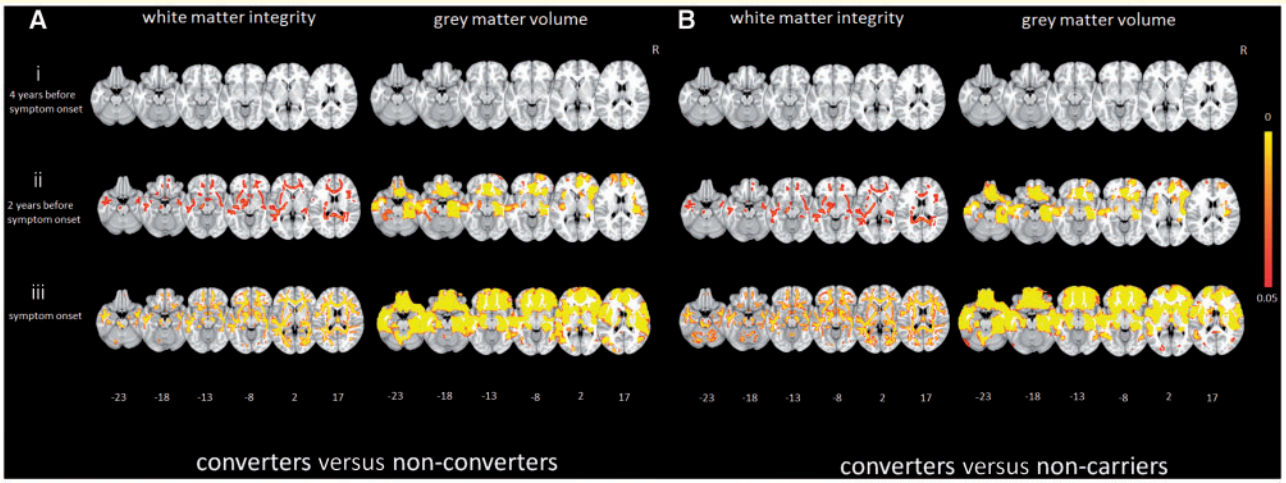

Figure 2 Cross-sectional whole brain grey matter volume and white matter integrity differences between converters, non-converters and non-carriers. Maps illustrate significant differences in white matter integrity (fractional anisotropy; *left*) and grey matter volume (*right*) between (**A**) converters and non-converters, and (**B**) between converters and non-carriers at (**i**) 4 years before onset; (**ii**) 2 years before onset; and (**iii**) at symptom onset. Fractional anisotropy thresholded ($P < 0.05$) statistical images were thickened using tbss_fill in FSL for better visibility. Colour bars represent *P*-values.

in the uncinate fasciculus, superior longitudinal fasciculus, inferior fronto-occipital fasciculus, inferior longitudinal fasciculus, corpus callosum, forceps minor, cingulum, anterior thalamic radiation and anterior corona radiata than both the other two groups [Table 2, Fig. 2A(ii) and B(ii)]. Lower grey matter volumes were found in the bilateral frontal and temporal lobes, insula and cingulate cortex, extending to the parietal lobe and cerebellum of converters compared to non-converters and non-carriers [Table 2 and Fig. 2A(ii)]. After symptom onset, converters had lower fractional anisotropy values across all white matter tracts [Table 2 and Fig. 2A(ii)], and lower grey matter volumes of large areas covering the frontal and temporal cortices, but also subcortical areas (e.g. thalamus) and cerebellum, with relative sparing of the parietal and occipital lobes in comparison to non-converters [Table 2 and Fig. 2A(ii)]. The differences were in similar locations, but more extensive in comparison to non-carriers [Table 2 and Fig. 2B(ii)]. The results were not affected by the converter with the cerebellar cyst, as exclusion did not change the above-mentioned findings. No significant differences in fractional anisotropy or grey matter volumes were found between non-converters and non-carriers at any time point (Table 2).

Longitudinal whole brain white matter integrity and grey matter volume loss

Converters demonstrated longitudinal decline of fractional anisotropy in the genu corpus callosum and forceps minor over time compared to non-converters (Table 2 and Fig. 3A); this was even more extensive (left uncinate fasciculus, left superior longitudinal fasciculus and posterior corpus callosum) when compared to non-carriers (Table 2 and Fig. 3A). The longitudinal trajectories of the right uncinate fasciculus and genu corpus callosum are shown in Fig. 4A. Furthermore, converters had significant grey matter volume loss of the prefrontal cortex, cingulate cortex, insula, temporal poles and inferior temporal gyrus in comparison to non-converters (Table 2 and Fig. 3B), again with more extensive grey matter volume loss (most of the frontal and temporal lobes, extending to the occipital cortex and cerebellum) compared to non-carriers (Table 2 and Fig. 3B). These results were also not affected by the converter with the cerebellar cyst, as exclusion did not change the above-mentioned findings. There were no significant differences in fractional anisotropy or grey matter volume loss between non-converters and non-carriers (Table 2).

Within-individual trajectories in converters

We further assessed the converters' within-individual progression of global cognitive (MMSE, FAB), neuropsychiatric (NPI-Q), neuropsychological (language, executive function, social cognition, attention, memory) and neuroimaging (frontal and temporal lobe volume) measures (Fig. 5). Furthermore, a brief description of the clinical disease trajectories, including the onset of behavioural, neuropsychiatric, cognitive and neuroimaging changes can be found in the Supplementary material. As Figs 4A, 5 and the Supplementary material show, most *MAPT* converters had a relatively gradual onset of symptoms, reflected in slowly progressive clinical features and cognitive disturbances, but a steep increase of neuropsychiatric and grey matter volume loss. The *GRN* converters

Downloaded from https://academic.oup.com/brain/article-abstract/142/1/193/5225004 by Erasmus University Rotterdam user on 07 January 2019

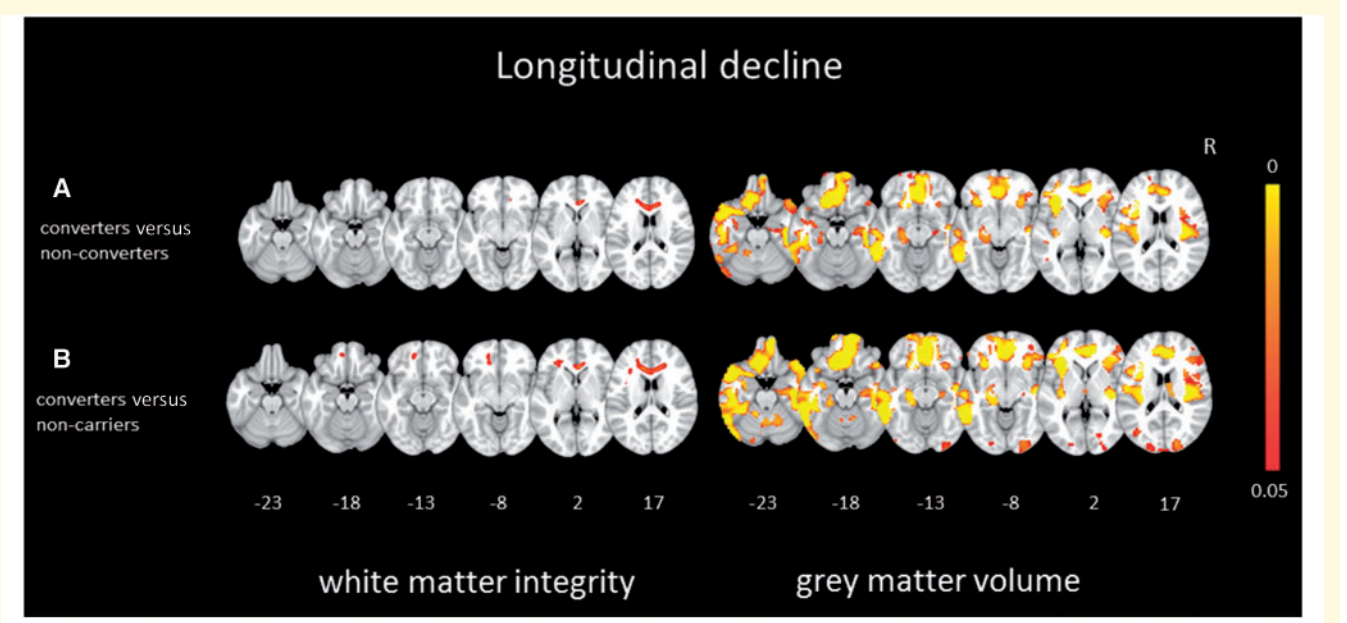

Figure 3 Longitudinal whole brain grey matter volume and white matter integrity differences between converters, non-converters and non-carriers. Maps illustrate significant differences in white matter integrity (*left*) and grey matter volume (*right*) between (**A**) converters and non-converters and (**B**) between converters and non-carriers. Fractional anisotropy thresholded ($P < 0.05$) statistical images were thickened using tbss_fill in FSL for better visibility. Colour bars represent *P*-values.

demonstrated more rapid changes in all biomarkers around symptom onset. With respect to cognition, *MAPT* converters demonstrated decline in all domains, namely language, attention, executive function, social cognition, and memory, while *GRN* converters declined most on attention and executive function (Supplementary Table 1 and Fig. 5). With respect to grey matter atrophy, visual inspection showed a disproportional volume loss of the (right) temporal lobes in *MAPT* converters, and relatively more volume loss of the (left) frontal lobes in *GRN* converters (Fig. 5). Visual inspection of the white matter trajectories suggested more fractional anisotropy decline in the uncinate fasciculus in *MAPT* converters than *GRN* converters, and more decline in the genu corpus callosum in *GRN* converters than *MAPT* converters (Fig. 4A). As most converters with bvFTD had an underlying *MAPT* mutation, similar patterns of decline were found; comparably, all converters with nfvPPA had an underlying *GRN* mutation, and therefore showed similar patterns of decline to *GRN* converters (Figs 4A and 5). A steep increase of neuropsychiatric symptoms was noted in most bvFTD converters (converter 1, 2, 4 and 8), but not in nfvPPA converters (Supplementary material and Fig. 5).

Classification

Between converters and non-converters, longitudinal decline in the white matter integrity of the right uncinate fasciculus and genu corpus callosum provided significant classifiers (Table 3 and Fig. 4B). Decline in the genu corpus callosum provided the best fit for classifying between converters and non-converters ($\chi^2 = 0.738$; $P < 0.001$). The model correctly classified 85.0% of cases. Between converters and non-carriers, longitudinal decline of the right uncinate fasciculus, genu corpus callosum, forceps minor, right inferior fronto-occipital fasciculus, right insula, and left anterior temporal lobe, provided significant classifiers (Supplementary Table 3 and Fig. 4B). Decline in the genu corpus callosum and right inferior longitudinal fasciculus provided the best fit for classifying between converters and non-carriers ($\chi^2 = 1.000$; $P < 0.001$). The model correctly classified 100% of cases.

Discussion

Our study is the first 4-year longitudinal study examining different neuroimaging modalities in a large cohort of at-risk participants from families with FTD due to *MAPT* or *GRN* mutations. Eight mutation carriers developed clinical features of FTD ('converters'). Cross-sectional analyses demonstrated extensive loss of white matter integrity and grey matter volume in converters, present from 2 years before symptom onset. Longitudinal analyses demonstrated the largest decline over time in the genu corpus callosum, uncinate fasciculus, forceps minor, and superior longitudinal fasciculus, as well as the prefrontal and cingulate cortex, insula, temporal pole and inferior temporal gyrus. Classifiers between converters, non-converters and non-carriers were white matter integrity loss of the right uncinate fasciculus and genu corpus callosum. Decline in the genu corpus callosum and right inferior longitudinal fasciculus

Downloaded from https://academic.oup.com/brain/article-abstract/142/1/193/5225004 by Erasmus University Rotterdam user on 07 January 2019

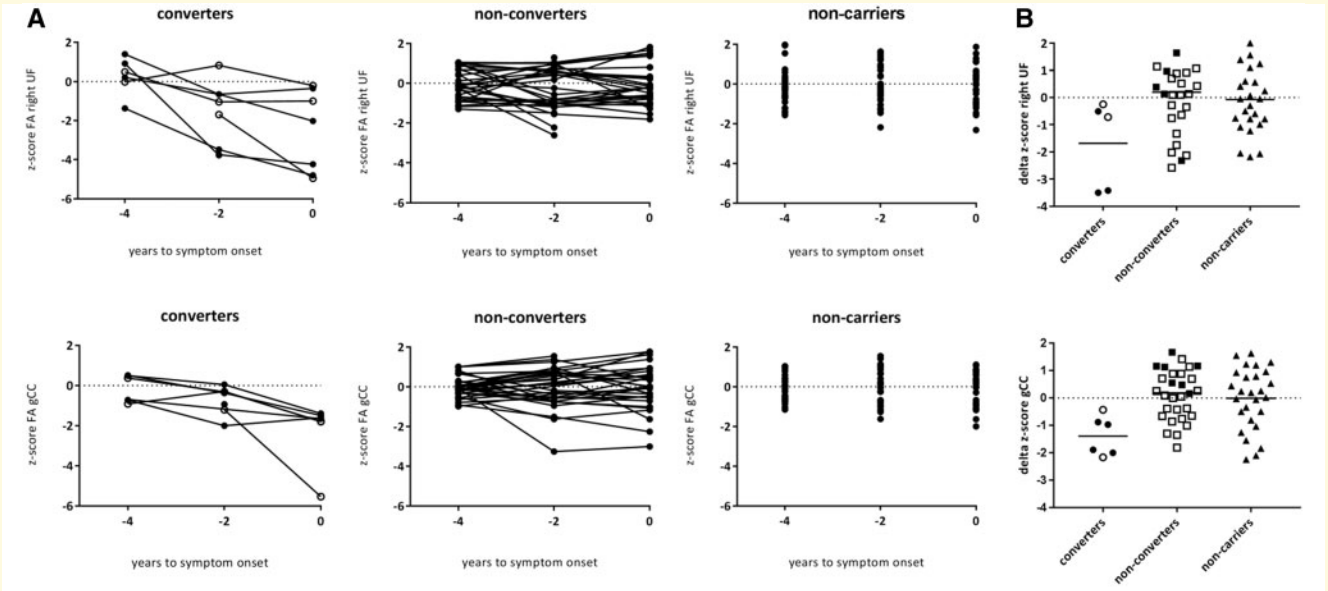

Figure 4 Longitudinal trajectories and classification accuracy of white matter integrity decline from the presymptomatic to symptomatic phase. (**A**) Longitudinal trajectories of white matter integrity (fractional anisotropy, FA) loss (z-score) in the right uncinate fasciculus (UF; *top row*) and genu of the corpus callosum (gCC; *bottom row*) in converters, non-converters and non-carriers. Open circles represent *GRN* converters; filled circles represent *MAPT* converters. Note that data points for two converters (one *MAPT*, one *GRN*) are missing at 4 years before symptom onset, as they converted between baseline and first follow-up, and therefore do not have the 4 years before symptom onset scan available. DTI data were of unsatisfactory quality for one (*MAPT*) converter 4 years before symptom onset (only uncinate fasciculus), and another (*MAPT*) converter 2 years before symptom onset (both uncinate fasciculus and genu of the corpus callosum) and were therefore excluded. Data were unavailable at symptom onset for one converter (*MAPT*) as the scan session was terminated prematurely. (**B**) Classification between converters, non-converters and non-carriers using the z-score delta fractional anisotropy of the right uncinate fasciculus (*top*) and the genu of the corpus callosum (*bottom*). The dashed line represents the optimal cut-off to separate converters and non-converters (uncinate fasciculus: delta fractional anisotropy = –0.51; sensitivity = 100%, specificity = 62.5%; genu of the corpus callosum: delta fractional anisotropy = –0.85; sensitivity = 100%, specificity = 81.3%). The optimal cut-off between converters and non-carriers (not shown) is –0.39 (sensitivity = 100%, specificity = 69.6%) and –0.87 (sensitivity = 100%, specificity = 91.3%) for the uncinate fasciculus and genu of the corpus callosum, respectively. Open circles represent *GRN* converters; filled circles represent *MAPT* converters. Note that deltas for two converters (one *MAPT*, one *GRN*) are missing, as they converted between baseline and first follow-up, and therefore do not have the 4 years before symptom onset scan available. DTI data of the uncinate fasciculus for one (*MAPT*) converter were excluded due to unsatisfactory quality.

provided the best measures for classifying between converters and non-converters.

Analogous to other cohort studies in familial FTD (Rohrer *et al.*, 2015), Alzheimer's disease (Bateman *et al.*, 2012; Benzinger *et al.*, 2013; Kinnunen *et al.*, 2018), and Huntington's disease (Tabrizi *et al.*, 2013; Harrington *et al.*, 2016), the transition period between presymptomatic and symptomatic disease stage, the time point of pathophysiological changes, type of progression and topographical order of neuroimaging changes, and genotype versus phenotype-specific patterns may give significant insights into the exact disease process of FTD; these are addressed below.

One of the key benefits of our study is the use of actual onset age in converters. Looking in more detail at symptom onset, converters with *GRN* mutations had a more sudden start of symptoms, while subtle behavioural and cognitive changes evolved over years in a few *MAPT* mutation carriers. Conversion was based on onset of clinical features of FTD (behavioural and/or language deterioration), significant functional decline, and neurocognitive deficits. All eight converters met the diagnostic criteria for probable bvFTD (Rascovsky *et al.*, 2011), or imaging-supported PPA (Gorno-Tempini *et al.*, 2011), as they had frontal and/or temporal atrophy consistent with patterns described in early-stage symptomatic *MAPT*- and *GRN*-related FTD (Whitwell *et al.*, 2009*b*, 2012; Rohrer *et al.*, 2010; Cash *et al.*, 2018). Although the present study does not include *C9orf72*-related FTD, it is important to recognize that symptomatic mutation carriers initially can have relatively normal structural imaging (Khan *et al.*, 2012; Devenney *et al.*, 2015) or atrophy patterns are less pronounced than in sporadic bvFTD (Devenney *et al.*, 2014); therefore using frontal and/or temporal MRI abnormalities as core criteria in defining clinical conversion could miss a proportion of mutation carriers if generalized to a cohort

Downloaded from https://academic.oup.com/brain/article-abstract/142/1/193/5225004 by Erasmus University Rotterdam user on 07 January 2019

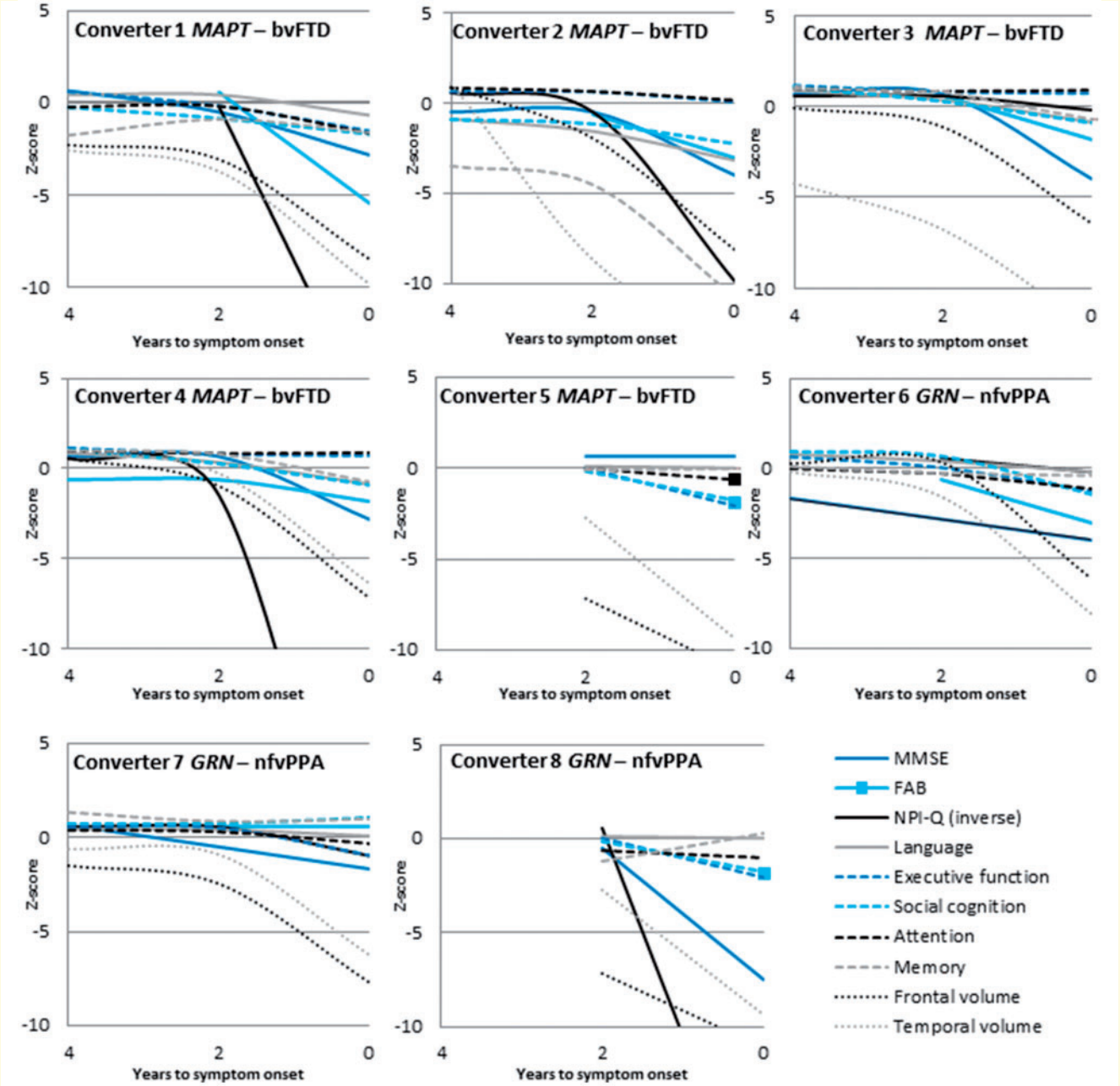

Figure 5 Within-individual trajectories of clinical and neuroimaging changes in converters. Raw data for each marker were first converted to z-scores by standardization to the baseline data of non-carriers. Each subplot (labelled with the converters number) presents the longitudinal global cognitive, neuropsychological and grey matter neuroimaging values (z-scores, *y*-axis) from 4 years to symptom onset to symptom onset (*x*-axis). The grey matter volumes of the most affected hemisphere are displayed (i.e. right side in converters with bvFTD, left side in all converters with nfvPPA). Coloured asterisks denote significant longitudinal decline ($\geqslant$ I SD) over time. FAB = Frontal Assessment Battery; MMSE = Mini-Mental State Examination.

including *C9orf72*. The exact timing of conversion was difficult to pinpoint due to a transitional stage of subtle behavioural or language impairment (Gorno-Tempini *et al.*, 2011; Rascovsky *et al.*, 2011), in line with the 'questionably/mildly symptomatic mutation carriers' described by Kinnunen *et al.* (2018). Analogous to the mild cognitive impairment (MCI) phase in Alzheimer's disease, several terms have been opted for this time period in FTD, such as 'pre-bvFTD' (Borroni *et al.*, 2015), 'prodromal frontotemporal dementia [FTD]' (Hallam *et al.*, 2007), 'frontotemporal MCI' (De Mendonça *et al.*, 2004) and the more broadly defined 'Mild Behavioural Impairment' (Taragano *et al.*, 2009). However, they do not capture the entire range of possible clinical features in presymptomatic familial

Downloaded from https://academic.oup.com/brain/article-abstract/142/1/193/5225004 by Erasmus University Rotterdam user on 07 January 2019

FTD, including early stage PPA. This emphasizes the need for additional clinical, neuroimaging, or fluid biomarkers. As a first step, incorporating neuropsychiatric measures into the definition of the transitional period of FTD could be considered, as subtle neuropsychiatric changes were found in presymptomatic mutation carriers in this and in previous studies (Rohrer *et al.*, 2015; Cheran *et al.*, 2018).

The most interesting findings of our study are the longitudinal changes in grey and white matter integrity 2 years before actual symptom onset, suggesting a specific 'change-point' when approaching symptom onset. A similar pattern was demonstrated regarding neuropsychological biomarkers in the same cohort (Jiskoot *et al.*, 2018*a*), with a sudden onset of cognitive decline in e.g. language, executive function, social cognition and memory from 2 years before symptom onset. Previous studies using estimated years to onset as a proxy demonstrated similar changes in grey matter volume (Rohrer *et al.*, 2015), white matter integrity (Jiskoot *et al.*, 2018*b*) and cognition (Jiskoot *et al.*, 2016), albeit earlier in the presymptomatic period, i.e. 5–10 years before estimated symptom onset. The discrepancy between the findings in our study and those in the larger GENFI study may be explained by the smaller and different samples (e.g. inclusion of *C9orf72* mutation carriers, all mutation carriers combined in one group), differences in analysis method (mixed-effects models versus ANCOVAs on changes over time maps, percentage of total intracranial volume versus corrected absolute volume), and the use of estimated years to onset versus actual symptom onset. Furthermore, when using cross-sectional data, inferences depend on the assumption that biomarker trajectories are similar across patients (Benzinger *et al.*, 2013), while in this study we were able to show that within-individual trajectories can differ. An interesting issue is the type of change (e.g. stepped change, linear) and rate of progression (e.g. gradual, accelerated) occurring after this change-point, and a study with a larger cohort of converters with longer follow-up will certainly shed more light on this matter. The present findings of a relatively rapid/abrupt trajectory of white and grey matter changes seems to be in contrast with that seen in familial Alzheimer's disease (Bateman *et al.*, 2012; Benzinger *et al.*, 2013). However, studies in familial Alzheimer's disease also show accelerated decline in the proximity of symptom onset (Hassenstab *et al.*, 2016; Kinnunen *et al.*, 2018), with disease rates being at least 3.6 times higher after the change-point (Kinnunen *et al.*, 2018). FTD, having shorter survival and faster rates of decline than Alzheimer's disease (Rascovsky *et al.*, 2005), could have an even faster rate of disease progression after the change-point.

The spatial distribution of grey matter and white matter changes 2 years before onset corresponds with significant loss of both white matter integrity and grey matter volume over time in symptomatic FTD (Frings *et al.*, 2014; Lam *et al.*, 2014; Mahoney *et al.*, 2014; Elahi *et al.*, 2017). The lower white matter integrity of the uncinate fasciculus in converters 2 years before symptom onset confirmed this tract as the molecularly most vulnerable hub, as also found in previous studies (Borroni *et al.*, 2008; Dopper *et al.*, 2014; Jiskoot *et al.*, 2018*b*). The involvement of several other tracts after symptom onset in our study supports the hypothesis of a network-led framework, in which neurodegeneration propagates along large-scale distributed white matter networks with disease progression (Seeley *et al.*, 2009). The spatial patterns of white matter integrity and grey matter volume loss revealed a strong co-localization, confirming some previous studies (Acosta-Cabronero *et al.*, 2011; Hornberger *et al.*, 2011), but contrasting with others (Agosta *et al.*, 2010, 2012; Mahoney *et al.*, 2013, 2014; Schwindt *et al.*, 2013; Zhang *et al.*, 2013). Although cross-sectional in nature, the cascade of presymptomatic grey matter changes found in the GENFI cohort (Rohrer *et al.*, 2015) was similar to the longitudinal patterns found in this study, with the atrophy spreading from the insula, temporal and frontal cortices to the cingulate, parietal and occipital cortices with approaching estimated symptom onset.

Prior studies have suggested that white matter abnormalities occur earlier and tend to exceed the grey matter atrophy (Agosta *et al.*, 2012; Rohrer and Rosen, 2013; Frings *et al.*, 2014; Lam *et al.*, 2014). We found relatively simultaneous onset of changes in white matter integrity and grey matter volume loss. The small number of converters did not allow us to detect a robust sequential order of grey and white matter involvement or between specific cortical regions, while more extensive progression of white matter pathology than grey matter abnormalities were found in longitudinal studies in the symptomatic stage (Frings *et al.*, 2014; Lam *et al.*, 2014). In our study, the progression of grey matter atrophy seems visually larger than the white matter integrity loss. Potentially, this does not occur initially in the presymptomatic stage, but later on in the disease process (Lam *et al.*, 2014). Our findings are in contrast with the more temporal order found in familial Alzheimer's disease, reflected in elevated amyloid [Pittsburgh compound B (PiB)] PET 15 years before estimated onset, followed by reduced glucose metabolism [fluorodeoxyglucose (FDG)-PET] 10 years before estimated onset, and cortical thinning 5 years before estimated onset (Benzinger *et al.*, 2013). As FDG-PET scanning has only been carried out in a small series of presymptomatic mutation carriers (Caroppo *et al.*, 2015), the use of FDG-PET in a larger cohort will definitively give more insights into the temporal sequence of pathophysiological changes. Analogous to PiB-PET scanning in Alzheimer's disease, the future availability of an optimal tau PET tracer in presymptomatic carriers with *MAPT* mutations will also give more information about the topographical and spatial spreading of tau pathology and its trajectory relative to grey matter atrophy and white matter integrity loss (Smith *et al.*, 2016; Ono *et al.*, 2017).

Regarding genotype-specific patterns of neuroimaging biomarkers, the uncinate fasciculus in *MAPT* converters tended to show the most decline in white matter integrity,

Downloaded from https://academic.oup.com/brain/article-abstract/142/1/193/5225004 by Erasmus University Rotterdam user on 07 January 2019

Table 3 Diagnostic performance of white matter integrity and grey matter volume loss between converters and non-converters

	L/R	AUC (95% CI)	*P*	Optimal cut-off	Sensitivity	Specificity
White matter tracts						
UF	R	0.83 (0.62–1.00)	**0.047**	–0.51	100%	62.5%
	L	0.81 (0.61–1.00)	0.059	-	-	-
SLF	R	0.72 (0.50–0.93)	0.186	-	-	-
	L	0.64 (0.31–0.97)	0.395	-	-	-
gCC	n/a	0.91 (0.86–1.00)	**0.014**	–0.85	100%	81.3%
bCC	n/a	0.59 (0.26–0.93)	0.571	-	-	-
sCC	n/a	0.72 (0.46–0.97)	0.186	-	-	-
Fornix	n/a	0.80 (0.54–1.00)	0.073	-	-	-
Forceps minor	n/a	0.73 (0.47–0.99)	0.156	-	-	-
Cingulum bundle	n/a	0.72 (0.36–1.00)	0.186	-	-	-
IFOF	R	0.77 (0.54–0.99)	0.108	-	-	-
	L	0.67 (0.41–0.94)	0.299	-	-	-
ILF	R	0.64 (0.37–0.91)	0.395	-	-	-
	L	0.63 (0.28–0.97)	0.450	-	-	-
Grey matter areas						
Frontal lobe	R	0.53 (0.22–0.84)	0.832	-	-	-
	L	0.66 (0.30–1.00)	0.235	-	-	-
Prefrontal cortex	R	0.52 (0.20–0.83)	0.899	-	-	-
	L	0.66 (0.31–1.00)	0.218	-	-	-
Temporal lobe	R	0.69 (0.35–1.00)	0.137	-	-	-
	L	0.61 (0.33–0.89)	0.396	-	-	-
ATL	R	0.51 (0.25–0.78)	0.932	-	-	-
	L	0.76 (0.47–1.00)	0.051	-	-	-
Insula	R	0.66 (0.38–0.94)	0.218	-	-	-
	L	0.60 (0.34–0.86)	0.445	-	-	-
Cingulate cortex	R	0.61 (0.31–0.91)	0.396	-	-	-
	L	0.78 (0.50–1.00)	**0.034**	–0.29	83.3%	86.7%
ACC	R	0.74 (0.37–0.92)	0.270	-	-	-
	L	0.65 (0.36–0.94)	0.252	-	-	-

ACC = anterior cingulate cortex; ATL = anterior temporal lobe; AUC = area under the curve; bCC = body corpus callosum; gCC = genu corpus callosum; IFOF = inferior fronto-occipital fasciculus; ILF = inferior longitudinal fasciculus; L = left; n/a = not applicable; R = right; sCC = splenium corpus callosum; SLF = superior longitudinal fasciculus; UF = uncinate fasciculus. White matter tract values represent fractional anisotropy, ranging between 0 and 1. Grey matter area values are expressed in millilitres, corrected for total intracranial volume. The optimal cut-off level was determined by the highest Youden's index (i.e. sensitivity + specificity − 1) (Youden, 1950). Significant *P*-values are given in bold.

and *GRN* converters showed the most decline in the genu corpus callosum, although the numbers in both groups were too low to perform statistical analyses in order to draw firmer conclusions. These findings are in line with reported white matter atrophy of the uncinate fasciculus in *MAPT*-associated FTD, and white matter atrophy of the corpus callosum in *GRN*-associated FTD (Rohrer *et al.*, 2010). Most of the *MAPT* converters in our study presented with bvFTD, which could explain the prominent involvement of the uncinate fasciculus, as reported earlier by Rohrer *et al.* (2010). Its role in both the language processing pathway (Grossman *et al.*, 2004) and its anatomical connections to the limbic system in the temporal lobe (Olson *et al.*, 2015) explains the strong connection between early damage to the uncinate fasciculus and the clinical phenotypes of *MAPT* and bvFTD, characterized by severe semantic and behavioural disturbances. With respect to grey matter atrophy, visual inspection showed more temporal volume loss in *MAPT* converters and frontal volume loss in *GRN* converters, in line with previous studies into both presymptomatic (Rohrer *et al.*, 2015) and symptomatic familial FTD (Whitwell *et al.*, 2009*b*, 2012; Cash *et al.*, 2018). Most of the *GRN* converters in our study presented with nfvPPA, in which the speech production impairments have been associated with prominent atrophy of the premotor cortex and the inferior frontal lobes (Rohrer *et al.*, 2013). With respect to disease progression, most converters with *MAPT* mutations had a slower progressive onset in clinical features, cognition, and grey matter atrophy and white matter integrity loss, indicating a more gradual disease progression. In contrast, all converters with *GRN* mutations had more rapid changes in these biomarkers around symptom onset, in line with a faster disease progression (Whitwell *et al.*, 2015) and atrophy occurring nearer to symptom onset (Cash *et al.*, 2018). Our results suggest variable disease trajectories between genetic mutation groups as well as within different genetic mutations, yet it remains to be elucidated whether the structural changes are solely phenotype-specific (bvFTD versus nfvPPA) changes, or whether they will follow genotypic patterns as well.

Downloaded from https://academic.oup.com/brain/article-abstract/142/1/193/5225004 by Erasmus University Rotterdam user on 07 January 2019

A larger cohort with more converters will provide us with more information on this matter, as—in contrast to amyloid-β in CSF and PIB-PET scans in Alzheimer's disease—there is a lack of pathophysiological-specific biomarkers for FTD.

The predictive value of changes in the uncinate fasciculus, genu corpus callosum and left cingulate cortex for conversion in the following 2 years is an important and novel finding, as multimodal studies into FTD are scarce (Zhang *et al.*, 2011). The finding of the genu corpus callosum as a significant discriminator between converters and non-converters is in line with the hypothesis of FTD as a network disease, in which loss of specific white matter tracts connecting grey matter areas results in large network failure. Studies into frontotemporal and Alzheimer's disease have demonstrated both unimodal white matter and grey matter volume loss as being significant discriminators between both conditions (albeit weaker for grey matter than white matter), but the optimal classification (87% sensitivity, 83% specificity) was achieved using a combination of techniques (McMillan *et al.*, 2012). Furthermore, Möller *et al.* (2015) showed that white matter integrity measures added complementary information to grey matter atrophy measures in FTD. It would be valuable for future studies to replicate the present classification findings, preferably with different and/or more neuroimaging techniques (e.g. resting state functional MRI, arterial spin labelling) or other statistical algorithms (e.g. support vector machines, machine learning techniques) to determine which combination of approaches could achieve the highest classification accuracy for conversion to the symptomatic disease stage.

With upcoming clinical trials, ongoing studies are investigating the potential of longitudinal MRI as sensitive disease biomarkers. These interventions should ideally be applied in the presymptomatic stage (Meeter *et al.*, 2017). For both white matter integrity and grey matter volume loss present at 2 years prior to symptom onset, and increasing pathology when moving into the symptomatic stage, multimodal neuroimaging has proven its value as a disease staging and tracking biomarker. Longitudinal DTI changes in the genu corpus callosum as the strongest predictor for conversion makes it a potential neuroimaging biomarker for tracking disease progression in clinical trials, particularly since this is the white matter tract most consistently found across all clinical FTD syndromes (Elahi *et al.*, 2017). Interestingly, the white matter integrity loss between 4 and 2 years before symptom onset seems to parallel the steep increase in neurofilament light chain levels found in converters in our previous study (Meeter *et al.*, 2016). Future research should focus on the association between DTI parameters and neurofilament light chain levels in a larger sample, as they could serve as potential biomarkers for disease staging, the prediction of underlying pathology, and monitoring of treatment response in future therapeutic trials. Moreover, investigating the white matter tract abnormalities underlying neuropsychiatric features in conversion to the symptomatic stage would be an informative next step, as recent research demonstrated distinct spatial distributions of white matter pathology to be associated with specific behavioural symptoms across the major clinical FTD syndromes (Lansdall *et al.*, 2018).

The key strength of our study is our longitudinal design, spanning a 4-year follow-up period of tracking at-risk participants from both *MAPT* and *GRN* families. The non-carriers from the same families were an ideal control group, as they had the same genetic and social background. Second, we used the true onset instead of estimated symptom onset. Third, all subjects underwent DTI imaging on the same scanner with the same sequencing parameters in a 4-year follow-up period. A drawback is the relatively small sample size and the clinical and pathological heterogeneity with respect to statistical power; this warrants replication in larger longitudinal cohorts with more converters, including *C9orf72* repeat expansion carriers. Although our cohort also involves participants from *C9orf72* families, study inclusion started in 2014; therefore no 5-year follow-up data are available yet. In the current study, we only described changes in fractional anisotropy, being the most sensitive parameter in the presymptomatic phase and the most pronounced measure with disease progression (Acosta-Cabronero *et al.*, 2012; Dopper *et al.*, 2014; Lam *et al.*, 2014). However, to interpret the exact neuropathological processes underlying the DTI changes, future studies should also include other diffusivity measures. Further, DTI scan-rescan reliability in neurodegeneration has scarcely been studied, and can be potentially hampered by its unequal distribution throughout different brain regions (i.e. highly anisotropic white matter tracts have lower within-subject variability) and higher susceptibility to partial volume effects in smaller tracts (Cole *et al.*, 2014). Finally, the DTI field-of-view in the present study was too small to include the lower white matter tracts in our analyses, although this would have been interesting considering recent findings of corticospinal tract degeneration in both bvFTD and nfvPPA (Omer *et al.*, 2017).

Conclusion

Our longitudinal study demonstrates the presence of presymptomatic structural neuroimaging changes in FTD mutation carriers, starting 2 years before onset, with predominant frontotemporal pathology spreading towards and into symptom onset. Presymptomatic decline of white matter integrity of the uncinate fasciculus and genu corpus callosum, and grey matter volume loss of the left cingulate cortex, are consistent predictors of symptom onset in converters. Our results confirm the presence of a presymptomatic neuroimaging stage of familial FTD, and highlight the potential value of longitudinal multimodal structural MRI as a sensitive prognostic and diagnostic biomarker for presymptomatic to early symptomatic familial FTD.

Downloaded from https://academic.oup.com/brain/article-abstract/142/1/193/5225004 by Erasmus University Rotterdam user on 07 January 2019

Acknowledgements

We would like to thank all participants and their families for taking part in our study.

Funding

This work was supported by the Dioraphte Foundation grant 09-02-03-00, the Association for Frontemporal Dementias Research Grant 2009, The Netherlands Organization for Scientific Research (NWO) grant HCMI 056-13-018, ZonMw Memorabel (Deltaplan Dementie, project number 733 051 042), Alzheimer Nederland and the Bluefield project. S.A. Rombouts is supported by NWO Vici grant number 016-130-677. L.H. Meeter is supported by Alzheimer Nederland (WE.09.2014-04).

Competing interests

The authors report no competing interests.

Supplementary material

Supplementary material is available at *Brain* online.

References

Acosta-Cabronero J, Patterson K, Fryer TD, Hodges JR, Pengas G, Williams GB, et al. Atrophy, hypometabolism and white matter abnormalities in semantic dementia tell a coherent story. Brain 2011; 134 (Pt 7): 2025–35.

Agosta F, Henry RG, Migliaccio R, Neuhaus J, Miller BL, Dronkers NF, et al. Language networks in semantic dementia. Brain 2010; 133: 286–99.

Agosta F, Scola E, Canu E, Marcone A, Magnani G, Sarro L, et al. White matter damage in frontotemporal lobar degeneration spectrum. Cereb Cortex 2012; 22: 2705–14.

Bateman RJ, Xiong C, Benzinger TLS, Fagan AM, Goate A, Fox N, et al. Clinical and biomarker changes in dominantly inherited Alzheimer's disease. N Engl J Med 2012; 367: 795–804.

Beck AT, Ward CH, Mendelson M, Mock J and Erbaugh J. An inventory for measuring depression. Arch Gen Psychiatry 1961; 4: 561–71.

Benzinger TLS, Blazey T, Jack CR Jr, Koeppe RA, Xiong C, Raichle ME, et al. Regional variability of imaging biomarkers in autosomal dominant Alzheimer's disease. Proc Natl Acad Sci USA 2013; 110: E4502–9.

Borroni B, Alberici A, Premi E, Archetti S, Garibotto C, Agosti C. Brain magnetic resonance imaging structural changes in a pedigree of asymptomatic progranulin mutation carriers. Rejuvenation Res 2008; 11: 585–95.

Borroni B, Cosseddu M, Pilotto A, Premi E, Archetti S, Gasparotti R, et al. Early stage of behavioural variant frontotemporal dementia: clinical and neuroimaging correlates. Neurobiol Aging 2015; 36: 3108–15.

Caroppo P, Habert MO, Durrleman S, Funkiewiez A, Perlbarq V, Hahn V, et al. Lateral temporal lobe: an early imaging marker of the presymptomatic GRN disease. J Alzheimers Dis 2015; 47: 751–9.

Cash DM, Bocchetta M, Thomas DL, Dick KM, van Swieten JC, Borroni B, et al. Patterns of gray matter atrophy in genetic frontotemporal dementia: results from the GENFI study. Neurobiol Aging 2018; 62: 191–6.

Cheran G, Silverman H, Manoochehri M, Goldman J, Lee S, Wu L, et al. Psychiatric symptoms in preclinical behavioural-variant frontotemporal dementia in MAPT mutation carriers. J Neurol Neurosurg Psychiatry 2018; 89: 449–55.

Cole JH, Farmer RE, Rees EM, Johnson HJ, Frost C, Scahill RI, et al. Test-retest reliability of diffusion tensor imaging in Huntington's disease. PLoS Curr 2014; 6. doi: 10.1371/currents.hd.f19ef63fff962f5cd9c0e88f4844f43b.

Cruchaga C, Fernández-Seara MA, Seijo-Martinez M, Samaranch L, Lorenzo E, Hinrichs A, et al. Cortical atrophy and language network reorganization associated with a novel progranulin mutation. Cereb Cortex 2009; 19: 1751–60.

De Mendonça A, Ribeiro F, Guerreiro M, Garcia C. Frontotemporal mild cognitive impairment. J Alzheimers Dis 2004; 6: 1–9.

Devenney E, Hornberger M, Irish M, Mioshi E, Burrell J, Tan R, et al. Frontotemporal dementia associated with the C9ORF72 mutation: a unique clinical profile. JAMA Neurol 2014; 71: 331–9.

Devenney E, Foxe D, Dobson-Stone C, Kwok JB, Kiernan MC, Hodges JR. Clinical heterogeneity of the C9orf72 genetic mutation in frontotemporal dementia. Neurocase 2015; 21: 535–41.

Dopper EG, Rombouts SA, Jiskoot LC, den Heijer T, de Graaf JR, de Koning I, et al. Structural and functional brain connectivity in presymptomatic familial frontotemporal dementia. Neurology 2014; 83: e19–26.

Dopper EG, Chalos V, Ghariq E, den Heijer T, Hafkemeijer A, Jiskoot LC, et al. Cerebral blood flow in presymptomatic *MAPT* and *GRN* mutation carriers: a longitudinal arterial spin labeling study. Neuroimage Clin 2016; 12: 460–5.

Dubois B, Litvan I. The FAB: a frontal assessment battery at bedside. Neurology 2000; 55: 1621–6.

Elahi FM, Marx G, Cobigo Y, Staggaroni AM, Kornak J, Tosun D, et al. Longitudinal white matter change in frontotemporal dementia subtypes and sporadic late onset Alzheimer's disease. Neuroimage Clin 2017; 16: 595–603.

Folstein MF, Folstein SE and McHugh PR. "Mini-mental state". A practical method for grading the cognitive state of patients for the clinician. J Psychiatr Res 1975; 12: 189–98.

Frings L, Yew, B, Flanagan E, Lam BY, Hüll M, Huppertz HJ, et al. Longitudinal grey and white matter changes in frontotemporal dementia and Alzheimer's disease. PLoS One 2014; 9: e90814.

Gorno-Tempini ML, Hillis AE, Weintraub S, Kertesz A, Mendez M, Cappa SF, et al. Classification of primary progressive aphasia and its variants. Neurology 2011; 76: 1006–14.

Grossman M, McMillan C, Moore P, Ding L, Glosser G, Work M, et al. What's in a name: voxel-based morphometric analyses of MRI and naming difficulty in Alzheimer's disease, frontotemporal dementia and corticobasal degeneration. Brain 2004; 127: 628–49.

Hallam BJ, Silverberg ND, Lamarre AK, Mackenzie IR, Feldman HH. Clinical presentation of prodromal frontotemporal dementia. Am J Alzheimers Dis Other Demen 2007; 22: 456–67.

Harrington DL, Long JD, Durgerian S, Mourany L, Koenig K, Bonner-Jackson A, et al. Cross-sectional and longitudinal multimodal structural imaging in prodromal Huntington's disease. Mov Disord 2016; 31: 1664–75.

Hassenstab J, Aschenbrenner AJ, Balota DA, Lim YY, McDade E, Wang G, et al. Cognitive trajectories in DIAN: relationships with symptom onset, mutation types and clinical status. Alzheimers Dement 2016; 12: 368.

Hornberger M, Geng J, Hodges JR. Convergent grey matter and white matter evidence of orbitofrontal cortex changes related to disinhibition in behavioural variant frontotemporal dementia. Brain 2011; 134: 2502–12.

Downloaded from https://academic.oup.com/brain/article-abstract/142/1/193/5225004 by Erasmus University Rotterdam user on 07 January 2019

Janssen JC, Schott JM, Cipolotti L, Fox NC, Scahill RI, Josephs KA, et al. Mapping the onset and progression of atrophy in familial frontotemporal lobar degeneration. J Neurol Neurosurg Psychiatr 2005; 76: 162–8.

Jiskoot LC, Dopper EG, Heijer T, Timman R, van Minkelen R, van Swieten JC, et al. Presymptomatic cognitive decline in familial frontotemporal dementia: a longitudinal study. Neurology 2016; 87: 384–91.

Jiskoot LC, Panman JL, van Asseldonk L, Franzen S, Meeter LHH, Donker Kaat L, et al. Longitudinal cognitive biomarkers predicting symptom onset in presymptomatic frontotemporal dementia. J Neurol 2018a; 265: 1381–92. doi: 10.1007/s00415-018-8850-7.

Jiskoot LC, Bocchetta M, Nicolas JM, Cash DM, Thomas D, Modat M, et al. Presymptomatic white matter integrity loss in familial frontotemporal dementia in the GENFI cohort: a cross-sectional diffusion tensor imaging study. Ann Clin Transl Neurol 2018b; 5: 1025–36.

Kaufer DI, Cummings JL, Ketchel P, Smith V, MacMillan A, Shelley T, et al. Validation of the NPI-Q, a brief clinical form of the neuropsychatric inventory. J Neuropsychiatry Clin Neurosci 2000; 12: 233–9.

Khan BK, Yokoyama JS, Takada LT, Sha SJ, Rutherford NJ, Fong JC, et al. Atypical, slowly progressive behavioural variant frontotemporal dementia associated with C9ORF72 hexanucleotide expansion. J Neurol Neurosurg Psychiatry 2012; 83: 358–64.

Kinnunen KM, Cash DM, Poole T, Frost C, Benzinger TLS, Ahsan RL, et al. Presymptomatic atrophy in autosomal dominant Alzheimer's disease: a serial magnetic resonance imaging study. Alzheimers Dement 2018; 14: 43–53.

Knopman DS, Kramer JH, Boeve BF, Caselli RJ, Graff-Radford NR, Mendez MF, et al. Development of methodology for conducting clinical trials in frontotemporal lobar degeneration. Brain 2008; 131: 2957–68.

Lam BYK, Halliday GM, Irish M, Hodges JR, Piguet O. Longitudinal white matter changes in frontotemporal dementia subtypes. Hum Brain Mapp 2014; 35: 3547–57.

Lansdall CJ, Coyle-Gilchrist ITS, Simon Jones P, Vázquez-Rodríguez P, Wilcox A, Wehmann E, et al. White matter change with apathy and impulsivity in frontotemporal degeneration syndromes. Neurology 2018; 90: e1066–76.

Mahoney CJ, Malone IB, Ridgway GR, Buckley AH, Downey LE, Golden HL, et al. White matter tract signatures of the progressive aphasias. Neurobiol Aging 2013; 34: 1687–99.

Mahoney CJ, Ridgway GR, Malone IB, Downey LE, Beck J, Kinnunen KM, et al. Profiles of white matter tract pathology in frontotemporal dementia. Hum Brain Mapp 2014; 35: 4163–79.

McMillan CT, Brun C, Siddiqui S, Churgin M, Libon D, Yushkevich P, et al. White matter imaging contributes to the multimodal diagnosis of frontotemporal lobar degeneration. Neurology 2012; 78: 1761–68.

Meeter LH, Donker Kaat L, Rohrer JD, van Swieten JC. Imaging and fluid biomarkers in frontotemporal dementia. Nat Rev Neurol 2017; 13: 406–19.

Meeter, LH, Dopper EGP, Jiskoot LC, Sanchez-Valle R, Graff C, Benussi L, et al. Neurofilament light chain: a biomarker for genetic frontotemporal dementia. Ann Clin Transl Neurol 2016; 3: 623–36.

Möller C, Hafkemeijer A, Pijnenburg YA, Rombouts SA, van der Grond J, Dopper E, et al. Joint assessment of white matter integrity, cortical and subcortical atrophy to distinguish AD from behavioral variant FTD: a two-center study. Neuroimage Clin 2015; 9: 418–29.

Mori S, Wakana S, Nagae-Poetscher LM, van Zijl PC. MRI atlas of human white matter. Amsterdam: Elsevier; 2005.

Oishi K, Faria A, Hsu J, Tippett D, Mori S, Hillis AE. The critical role of the right uncinate fasciculus in emotional empathy. Ann Neurol 2015; 77: 68–74.

Olson IR, von der Heide RJ, Alm KH, Vyas G. Development of the uncinate fasciculus: implications for theory and developmental disorders. Dev Cogn Neurosci 2015; 14: 50–61.

Omer T, Finegan E, Hutchinson S, Doherty M, Vajda A, McLaughlin RL, et al. Neuroimaging patterns along the ALS-FTD spectrum: a multiparametric imaging study. Amyotroph Lateral Scler Frontotemporal Degener 2017; 18: 611–23.

Ono M, Sahara N, Kumata K, Ji B, Ni R, Koga S, et al. Distinct binding of PET ligands PBB3 and AV-1451 to tau fibril strains in neurodegenerative tauopathies. Brain 2017; 140: 764–80.

Piguet O, Hornberger M, Mioshi E, Hodges JR. Behavioural variant frontotemporal dementia: diagnosis, clinical staging, and management. Lancet Neurol 2011; 10: 162–72.

Rascovsky K, Hodges JR, Knopman D, Mendez MF, Kramer JH, Neuhaus J, et al. Sensitivity of revised diagnostic criteria for the behavioural variant of frontotemporal dementia. Brain 2011; 134: 2456–77.

Rascovsky K, Salmon DP, Lipton AM, Leverenz JB, DeCarli C, Jagust WJ, et al. Rate of progression differs in frontotemporal dementia and Alzheimer disease. Neurology 2005; 65: 397–403.

Rohrer JD, Nicholas JM, Cash DM, van Swieten JC, Dopper EGP, Jiskoot LC, et al. Presymptomatic cognitive and neuroanatomical changes in genetic frontotemporal dementia in the Genetic Frontotemporal dementia Initiative (GENFI) study: a cross-sectional analysis. Lancet Neurol 2015; 14: 253–62.

Rohrer JD, Ridgway GR, Modat M, Ourselin S, Mead S, Fox NC, et al. Distinct profiles of brain atrophy in frontotemporal lobar degeneration caused by progranulin and tau mutations. NeuroImage 2010; 53: 1070–6.

Rohrer JD, Rosen HJ. Neuroimaging in frontotemporal dementia. Int Rev Psychiatry 2013; 25: 221–9.

Ryman DC, Acosta-Baena N, Aisen PS, Bird T, Danek A, Fox NC, et al. Symptom onset in autosomal dominant Alzheimer disease: a systematic review and meta-analysis. Neurology 2014; 83: 253–60.

Schuster C, Elamin M, Hardiman O, Bede P. Presymptomatic and longitudinal neuroimaging in neurodegeneration—from snapshots to motion picture: a systematic review. J Neurol Neurosurg Psychiatry 2015; 86: 1089–96.

Seeley WW, Crawford R, Rascovsky K, Kramer JH, Weiner M, Miller BL, et al. Frontal paralimbic network atrophy in very mild behavioral variant frontotemporal dementia. Arch Neurol 2008; 65: 249–55.

Seeley WW, Crawford RK, Zhou J, Miller BL, Greicius MD. Neurodegenerative diseases target large-scale human brain networks. Neuron 2009; 62: 42–52.

Schwindt GC, Graham NL, Rochon E, Tang-Wai DF, Lobaugh NJ, Chow TW, et al. Whole-brain white matter disruption in semantic and nonfluent variants of primary progressive aphasia. Hum Brain Mapp 2013; 34: 973–84.

Smith R, Puschmann A, Schöll M, Ohlsson T, van Swieten JC, Honer M, et al. ^{18}F-AV-1451 tau PET imaging correlates strongly with tau neuropathology in MAPT mutation carriers. Brain 2016; 139: 2372–9.

Tabrizi SJ, Scahill RI, Owen G, Durr A, Leavitt BR, Roos RA, et al. Predictors of phenotypic progression and disease onset in premanifest and early-stage Huntington's disease in the TRACK-HD study: analysis of 36-month observational data. Lancet Neurol 2013; 12: 637–49.

Taragano FE, Allegri RF, Krupitzki H, Sarasola DR, Serrano CM, Lon L, et al. Mild behavioural impairment and risk of dementia: a prospective cohort study of 358 patients. J Clin Psychiatry 2009; 70: 584–92.

van Swieten JC, Heutink P. Mutations in progranulin (GRN) within the spectrum of clinical and pathological phenotypes of frontotemporal dementia. Lancet Neurol 2008; 7: 965–74.

Verhage F. Intelligence and age: study with Dutch People Aged 12–77. Assen: van Gorcum; 1964.

Warren JD, Rohrer JD, Rossor MN. Clinical review. Frontotemporal dementia. BMJ 2013; 347: f4827.

Whitwell JL, Przybelski SA, Weigand SD, Ivnik RJ, Vemuri P, Gunter JL, et al. Distinct anatomical subtypes of the behavioural variant of

Downloaded from https://academic.oup.com/brain/article-abstract/142/1/193/5225004 by Erasmus University Rotterdam user on 07 January 2019

frontotemporal dementia: a cluster analysis study. Brain 2009a; 132: 2932–46.
Whitwell JL, Jack CR, Boeve BF, Senjem ML, Baker M, Rademakers R, et al. Voxel-based morphometry patterns of atrophy in FTLD with mutations in MAPT or PGRN. Neurology 2009b; 72: 813–20.
Whitwell JL, Weigand SD, Boeve BF, Senjem ML, Gunter JL, DeJesus-Hernandez M, et al. Neuroimaging signatures of frontotemporal dementia genetics: C9ORF72, tau, progranulin and sporadics. Brain 2012; 135: 794–806.
Whitwell JL, Boeve BF, Weigand SD, Senjem ML, Gunter JL, Baker MC, et al. Brain atrophy over time in genetic and sporadic frontotemporal dementia: a study of 198 serial magnetic resonance images. Eur J Neurol 2015; 22:745–52.
Youden WJ. Index for rating diagnostic tests. Cancer 1950; 3: 32–5.
Zhang Y, Tartaglia MC, Schuff N, Chiang GC, Ching C, Rosen HJ, et al. MRI signatures of brain macrostructural atrophy and microstructural degradation in frontotemporal lobar degeneration subtypes. J Alzheimers Dis 2013; 33: 431–44.
Zhang Y, Schuff N, Ching C, Tosun D, Zhan W, Nezamzadeh M, et al. Joint assessment of structural, perfusion, and diffusion MRI in Alzheimer's disease and frontotemporal dementia. Int J Alzheimers Dis 2011; 2011: 546–71.

Downloaded from https://academic.oup.com/brain/article-abstract/142/1/193/5225004 by Erasmus University Rotterdam user on 07 January 2019